

A modular localization system combining passive RF detection and passive radar

Markus Krueckemeier, Fabian Schwartau and Joerg Schoebel
Technische Universität Braunschweig, Institut für Hochfrequenztechnik, Microwave Engineering Lab
38106 Braunschweig, Germany
markus.krueckemeier@ihf.tu-bs.de

Abstract—This paper presents a completely passive system for detection and localization of small aircraft and UAVs. The system makes use of the fact that almost any such target emits some kind of RF emission, either by active transmissions or by passive reflection of other sources. Active transmissions can for example be caused by telemetry or video downlinks to a remote control or some kind of unintended emission like a mobile phone carried by a passenger. These transmissions can be identified by means of passive detection. At the same time, passive reflections of signals radiated by illuminators of opportunity like FM radio stations can be used to build a multistatic passive radar.

I. INTRODUCTION

Our RF based source localization system is projected to fuse passive detection and passive radar capabilities into one software-defined hardware platform. The idea behind the system is that an aircraft or UAV will be detectable with a high probability by means of RF signals, which could either be emitted by the target itself or could just be reflections from illuminators of opportunity. The type of the emissions or signals can be differentiated into three groups: The first group are active transmissions, which can either be required for the operation of the target or be unintentional. These will encompass video downlinks used for long-range remote controlled drones, or active WI-FI or mobile radio connections on-board of the target. This information can be used for the detection of a target and will also add attributes for the classification. The second group are backscattered signals, which originate from existing radio systems, like FM broadcast radio stations. Utilizing these signals as illuminators of opportunity, the system will provide passive radar capabilities [1]. The third group are broadcast information, like ADS-B, which includes the GPS coordinates of the target. These types of intentional broadcasts include all necessary information for the localization and classification of a target and can be used to verify the analysis of other measurements. To exploit any of these signals, the hardware is projected as a wideband RF receiver with multiple, synchronized inputs, a switchable antenna matrix and a powerful digital signal processing unit. By utilizing the advantages of digital signal processing, the hardware can be used as a platform for various applications, like multiband RF detection and passive radar applications. The presented sensor system is developed as a part of the ALFA System [2], which contains other sensors, like active

©2019 IEEE

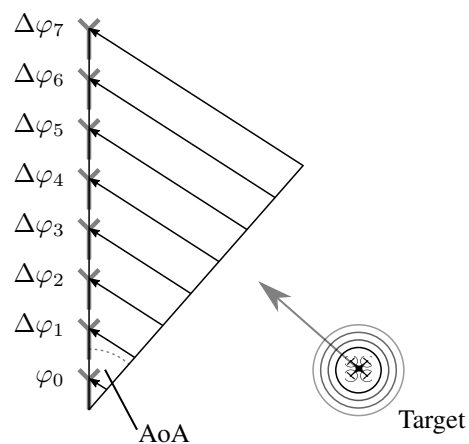


Fig. 1. Illustration of the AoA measurement principle

radar and electro optical sensors, a data fusion component and a user interface.

II. RF LOCALIZATION

The main principle of both RF detection and passive radar is the ability of the system to measure the direction of an incoming radio signal. In the case of the RF detection this signal is actively transmitted by the target. For the passive radar it is the reflection of a signal transmitted by a transmitter of opportunity. In both cases the signal can be described as a planar, electromagnetic wave front originating from the target and propagating towards the receiver. The AoA (Angle of Arrival) of such a wavefront can be determined with a delay and sum beamformer [3, p. 23-31]. Since the observed signals have a rather small bandwidth, the implementation is carried out using phase shifts instead of true time delays, reducing the needed computational effort. The principal is illustrated in fig. 1 with the example of an ULA (Uniform Linear Array) antenna.

III. SYSTEM DESCRIPTION

The core hardware component of the presented system is a fully coherent 8-channel software defined radio (SDR), which is capable of receiving signals from 10 MHz to 6 GHz with up to 80 MHz of simultaneously sampled bandwidth. To support multiple antenna arrays for different bands, the system includes switchable LNA front-ends, which can be controlled

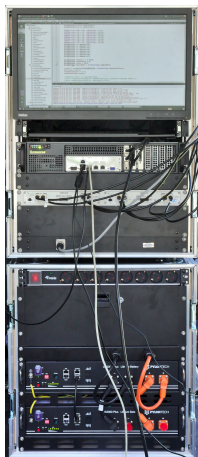


Fig. 2. SDR system, including synchronization and power supply

directly by the SDR hardware to support fast switching. These front-ends can also be utilized to calibrate the receiver chain. To achieve the versatility needed for the system, the signal processing is made in the digital domain. The conversion from the analog receive signal to a digital data stream is performed with two synchronized Ettus X310 software defined radios, equipped with four TwinRX daughterboards [4]. This results in an 8-channel coherent software defined receiver. Since the total frequency range cannot be covered with a single antenna array, a modular, cascadable approach, consisting of multiple, switchable antenna arrays was devised. The switching between the arrays is controlled by the USRPs, using the programmable GPIO connector. The GPIO output is converted to RS485 commands that ultimately control the analog front-end. The use of a serial bus allows the supply of the antenna component with a single four-wire cable. A block diagram of the RF setup is depicted in figure 3. For each antenna in each array there is a switch that allows to change the input either to the antenna, or to the next higher array, or to a calibration signal. The signal processing back-end is a high-performance computer with an Intel Xeon CPU, 64 GByte RAM and a graphics card with CUDA processing capabilities. To handle the vast amount of raw data generated by the USRPs, the link to the signal processing back-end is accomplished with two 10 Gigabit Ethernet connections. For further optimization of the signal processing it would also be possible to utilize the FPGAs of the USRPs for pre-processing of the raw data. The realized system is shown in figure 2. The lower case houses a battery supply for outdoor measurements, the upper case houses the actual system.

IV. ANTENNAS

Generally, the distance between the antenna elements in an array imposes a boundary to the bandwidth of the array. To avoid ambiguities in the angle determination, the distance has to be approximately a half wavelength at the highest frequency of the array. This reduces the gain at lower frequencies and increases mutual coupling, so that the properties of the

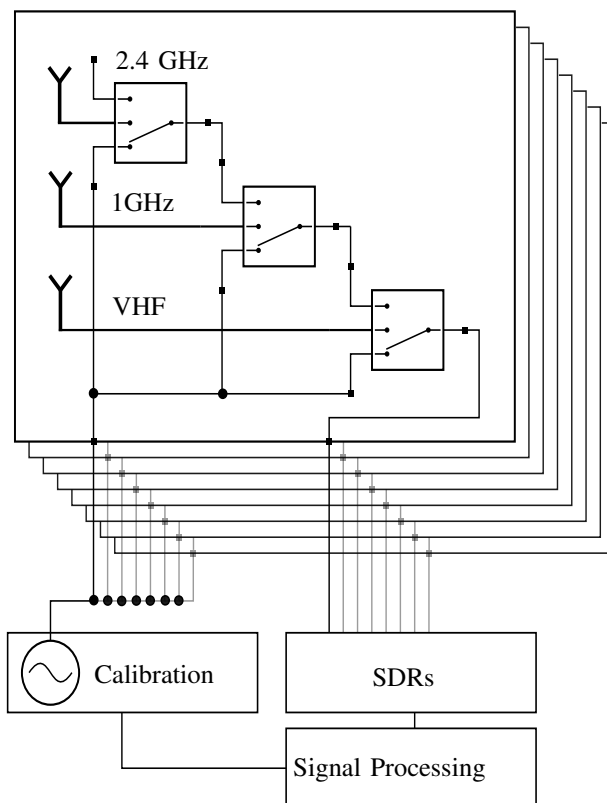


Fig. 3. Block diagram of the complete system

antenna array deteriorate. Hence, the bandwidth of an array is practically limited even if the antenna elements exhibit a rather wide bandwidth. Since the receiver system supports a large frequency range, the system was designed to support up to sixteen different arrays simultaneously, by equipping them with the switchable RF front-end. The system currently includes three antenna arrays; a circular VHF array and two linear arrays for 800 MHz to 1.1 GHz and the 2.4 GHz ISM-band. The VHF array is used for FM passive radar and the localization of aeronautical radio service. The first linear array covers frequencies for a common mobile communication band and secondary radar transponders used for air traffic control. The second linear array covers most UAV control and telemetry links, as well as Wi-Fi. The presented system could easily be expanded to cover further bands. The complete antenna setup is shown in Fig. 4.

V. RF FRONT-ENDS

To achieve the modular, cascadable antenna component, a controllable RF front-end was devised. The main component of the RF front-end is a 3:1 signal switch. One input is used as a link to the next antenna array, another one connects



Fig. 4. VHF circular array with two linear arrays for 1 GHz and 2.4 GHz on top

to a distributed calibration signal. The third input is used for the antenna input. On this port an additional low noise amplifier is installed. The amplifier input is protected with a bandpass filter to avoid a desensitization by interfering signals in other bands. The hardware consists of two PCBs, as can be seen in the block diagram in figure 5. One PCB is a generic communication, control and power supply unit, common for all front-ends. It assures a galvanic isolation to the rest of the system, produces the supply voltages for the RF board and handles the RS485 communication with the main system. The RS485 bus together with the power supply is serially connected from each board to the next via a 4-wire interface. The received commands are transformed to control signals for the RF board. The second board houses the filter, low noise amplifier and RF switch. The amplifier is designed for a bandwidth between 50 MHz and 6 GHz. The input filter is interchangeable with any filter in a Minicircuits FV1206-4 case, which allows for customization of the HF board for different frequency bands. Each board has an unique 7-bit ID, which consists of four bits assigning the array and three bits to address each antenna individually. This leads to a maximum of sixteen arrays that can be used simultaneously.

VI. SOFTWARE

The software on the system is built on the foundation of the hardware control component. On initialization the interface

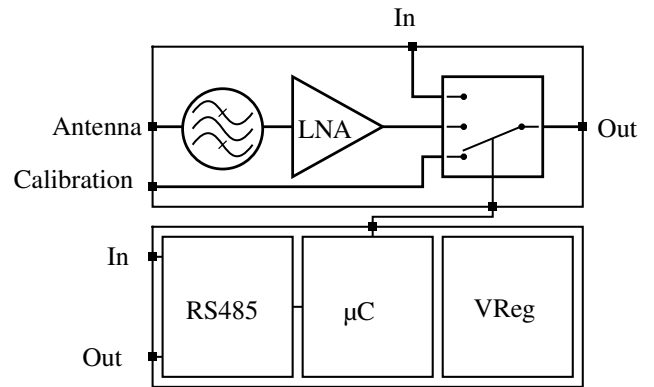


Fig. 5. Block diagram of the RF front-end

with the SDRs is established and a general configuration is loaded. The main task of this component is to configure the system for different frequency bands and forward the collected samples to higher level detector tasks. To ensure the synchronicity between the eight channels, each command like switching the frequency, changing the gain or starting a measurement is prepared in advance and sent to both USRPs together with a timestamp for the execution. The received data is put into a common structure and passed to the specialized detectors for further processing.

The system currently offers two basic detectors, an FM radio based passive radar and a passive RF detector. For the passive RF detection of (un-)intentional emissions from a target, the signal is converted to the frequency domain with a Fourier transform. Based on the power average of all eight antennas an adaptive noise level is calculated. This noise level is used to detect frequency ranges with more power than the usual noise level, which are declared as emissions. Targets are then defined by grouping together these emissions with no or small gaps in between them. Each target is then cut from the spectrum and fed into a beamforming algorithm to determine the angle of arrival, its total power and other features.

For the passive radar subsystem FM radio broadcast stations were chosen as the illuminators of opportunity. These stations transmit at high powers at rather low frequencies, leading to a good illumination coverage. Furthermore, the different stations, available at a location, are usually not operated on the same frequency, which means in terms of passive radar a mitigation of the risk of ambiguous detections. The signal processing for FM passive radio also starts with a Fourier transform of the eight receiver channels. The first channel is the reference channel from the antenna mounted at the top of the mast, which is horizontally polarized, just like the transmitters. This channel will receive a relatively clean reference signal with only the delay from the line-of-sight path from the transmitter to the receiver. The other seven channels are vertically polarized to make direct path coupling to these channels as low as possible. As reflections from airplanes and other targets are often a result of reflections from multiple surfaces at different angles, it is likely that a

polarization rotation is induced. Therefore, the received signal strength from the target is more or less independent of the receiving antennas' polarization. The reference channel still contains reflections from static targets like large buildings or mountains. To reduce these reflections the Constant Modulus Algorithm (CMS) is used [5]. This algorithm utilizes the fact that the amplitude (modulus) of a frequency modulated signal is constant. Delayed reflections of nonmoving objects will induce a varying amplitude due to multipath effects. The algorithm is able to estimate an FIR (finite impulse response) filter that will flatten the amplitude of the signal, thus removing echoes from the reference signal. The seven surveillance channels are subject to strong interference (signals that are not reflections from the targets). The by far strongest interference is the coupling of the line-of-sight path into the antennas. Although they are of different polarization, it is typical to have coupling of more than 20 dB over to the surveillance channels. Additionally, reflections from static objects induce even more clutter. To reduce both types of interference, a normalized least mean squares (NLMS) algorithm is used [6]. The NLMS algorithm is usually used for noise suppression. In our case we use it to continuously estimate an FIR filter that tries to reconstruct each surveillance channel with the cleaned reference signal as input. The filter is thus able to reproduce the direct path coupling and clutter. As the targets usually have a Doppler shift, the filter is not able to reproduce those. After subtracting the reconstructed signal from the surveillance channel (under ideal conditions) only the targets will remain. The clean reference signal and the seven surveillance channels with applied NLMS to each are then used to calculate a range-Doppler matrix. Therefore, the signals are split into smaller parts and the cross-correlation between each time block is calculated. The resulting fast-time impulse responses are then packed into a matrix, one impulse response per row. An FFT over the slow-time axis (across multiple impulse responses) converts the matrix into a range-Doppler matrix.

VII. MEASUREMENTS

An exemplary passive detection is shown in Fig. 6. In this case the 2.4 GHz band was observed; the spectrum is visible in the top left corner of Fig. 6. Below the spectrum is a representation that plots the power over angle and frequency. On the right side is a map representation, in which the detections are marked with lines. In this case an active Wi-Fi connection was measured (blue line) and the video downlink of a DJI Mavic Pro UAV was detected (red line).

Fig. 7 shows a range-Doppler matrix generated with the passive radar detector. The image shows four detected targets, which are marked with blue circles. The black crosses represent the range-Doppler values that were calculated for the targets found in the simultaneously recorded ADS-B data, which provide a validation of the passive radar detections. The large amplitude around zero Doppler and zero range is caused by very small variations in the clutter, which cannot be compensated, and is thus ignored. A detection at zero Doppler

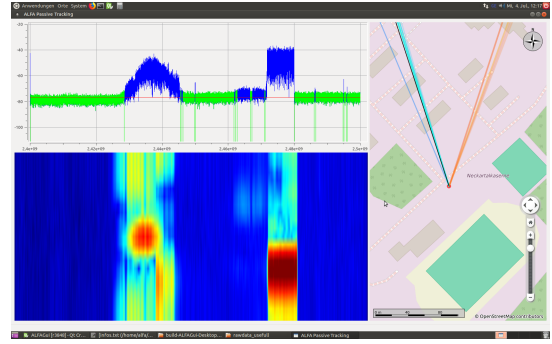


Fig. 6. Screenshot of the GUI during a demonstration. A Wi-Fi access point and the video downlink from an UAV were detected

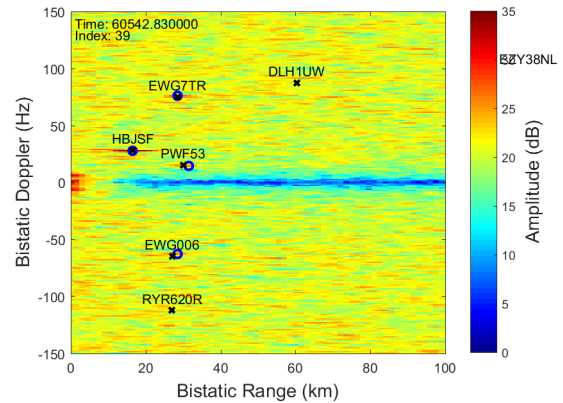


Fig. 7. Range-Doppler matrix overlaid with range doppler information calculated from ADS-B data

is in general not possible, as a target with zero Doppler is not distinguishable from static clutter.

ACKNOWLEDGEMENTS

This work was carried out in the scope of the ALFA project, which has received funding from the European Union's Horizon 2020 programme under grant agreement No. 700002.

REFERENCES

- [1] M. Malanowski, K. Kulpa, and J. Misiurewicz, "Parade-passive radar demonstrator family development at warsaw university of technology," in 2008 *Microwaves, Radar and Remote Sensing Symposium*. IEEE, 2008, pp. 75–78.
- [2] <https://alfa-h2020.eu/>.
- [3] H. L. Van Trees, *Optimum array processing: Part IV of detection, estimation, and modulation theory*. John Wiley & Sons, 2004.
- [4] M. Krueckemeier, F. Schwartz, C. Monka-Ewe, and J. Schoebel, "Synchronization of multiple usrp sdrs for coherent receiver applications," in 2019 *Sixth International Conference on Software Defined Systems (SDS)*. IEEE, 2019, pp. 11–16.
- [5] J. Benesty and P. Duhamel, "Fast constant modulus adaptive algorithm," *IEE Proceedings F - Radar and Signal Processing*, vol. 138, no. 4, pp. 379–387, Aug 1991.
- [6] M. E. Domnguez, W. Hernandez, and G. Sansigre, "General block lms algorithm," in 2009 *35th Annual Conference of IEEE Industrial Electronics*, Nov 2009, pp. 3371–3374.